International Journal of GEOMATE, March., 2023, Vol.24, Issue 103, pp.26-33
ISSN: 2186-2982 (P), 2186-2990 (O), Japan, DOI: https://doi.org/10.21660/2023.103.3426
Geotechnique, Construction Materials and Environment

IDENTIFICATION OF GEOLOGICAL STRUCTURES IN SIGI REGENCY, CENTRAL SULAWESI BASED ON DERIVATIVE ANALYSIS OF GRAVITY DATA

*Mohammad Syamsu Rosid[1], Saskia Nursarifa[1], and Agus Riyanto[1]

[1]Faculty of Mathematics and Sciences, Universitas Indonesia, Depok 16424, Indonesia

*Corresponding Author, Received: 22 April 2022, Revised: 02 Dec. 2022, Accepted: 10 Feb. 2023

ABSTRACT: Sigi Regency is part of the tectonic zone in Central Sulawesi which is crossed by an active transform fault, the Palu Koro Fault. The northern region of Sigi Regency has a depression zone that forms a graben by a couple of Palu Koro Faults. The study area is prone to earthquakes and has fairly high geothermal potential. Therefore, it is necessary to control the dynamics of the structure here to mitigate earthquake disasters that may occur and may also affect the surrounding geothermal system. To identify the presence and characterization of the fault structures, derivative analysis of gravity data is used, including analysis of FHD (First Horizontal Derivative), SVD (Second Vertical Derivative), and MS-SVD (Multi Scale-Second Vertical Derivative). From this analysis, 4 normal oblique fractures and 1 normal fracture were identified. Faults derived from the derivative analysis have greatly improved the fault mapping reported on geological maps, including the shifting fault position from the geological map. And significant improvement was found on a shear fault causing the fault to be separated into 2 segments, changing the direction of the strike fault, and generating a new fault due to the created weak zone.

Keywords: Palu Koro Fault, Gravity data, MS-SVD, Sigi Regency

1. INTRODUCTION

Sigi Regency is geographically located on Sulawesi Island, Indonesia at coordinates 1.4 ºS 120 ºE. This area is right south of Palu City, Central Sulawesi. Sulawesi Island, in general, is at the confluence of three large plates: the Eurasian plate, the Indo-Australian plate, and the Pacific plate [1]. This tectonic activity has produced many faults, one of which is the main and regional Palu Koro Fault (PKF), and related volcanic activities. Like Palu City, Sigi Regency is a tectonic zone that is crossed by an active fault of the Palu Koro Fault. The slip rate of the Palu Koro Fault is reported at around 20–40 millimeters per year [2-5]. The northern region of Sigi Regency is in a depression zone controlled by the tectonic activity of the Palu Koro Fault and surrounding normal faults [6]. Tectonic activities and a fault zone is an unstable zone and may cause occurring earthquakes.

In 1909 there was an earthquake in the graben area of Palu and in 2018 an earthquake and liquefaction occurred in parts of the Sigi Regency [7, 8]. The 2018 Palu earthquake with a magnitude of 7.4 Mw, has shaken Sigi up to VII-VIII MMI (modified Mercalli intensity) [9]. Sigi Regency is included in the strong Coulomb stress zone for the 2018 Palu earthquakes [10, 11]. The Sigi area in particular has also experienced two quite large earthquakes in 2012 and 2020 with respective strengths of M 6.2 and M 5.8. However, it is believed that the two earthquakes were not triggered by the activity of the Palu Koro Fault, but allegedly due to the activity of the Lore Lindu Fault which is 8 km east of the Palu Koro Fault and trending west-east perpendicular to the Palu Koro Fault [12]. Therefore, in the Sigi area, it is necessary to carry out a more comprehensive fault study to anticipate seismic disasters that may occur. Moreover, the dynamics of the fault structure can also influence and control the geothermal system around the study area.

Sulawesi is one of the areas with geothermal potential in Indonesia which is dominated by non-volcanic geothermal with low to moderate enthalpy [13-16]. One of the geothermal fields that have been proven is Lahendong in North Sulawesi [17, 18]. Sigi Regency also has geothermal potential which is indicated by manifestations of hot springs [6, 19-21]. Even some results of a preliminary studies in geophysics (such as magnetotelluric, and gravity) and geochemistry have confirmed the geothermal potential in the Sigi area [22-25]. One of the main geothermal parameters is the presence of fault structures as an indicator of a secondary permeable zone.

Unfortunately, there has been no previous study that comprehensively mapped the fault structures in the Sigi area. It was only reported the geomorphology and lithology of the rock [26]. Even if they mention the structure of the fault, researchers only allude to and more interest to the main Palu

Koro Fault [26, 27]. The existence of local faults is also important to observe for both disaster mitigation and geothermal exploration. Therefore, it is necessary to investigate the presence of fault structures in Sigi area in detail. FHD (First Horizontal Derivative), SVD (Second Vertical Derivative), and MS-SVD (Multi Scale-Second Vertical Derivative) methods have been widely used to characterize fault structures such as strike direction, fault type, magnitude, and dip direction of the structures [28, 29]. This study aims to identify and characterize the presence of fault structures in the study area.

2. RESEARCH SIGNIFICANCE

This study is very useful for earthquake disaster mitigation to anticipate the adverse effects caused by unstable fault zones. Identification of this fault structure is also useful for determining the potential of the geothermal reservoir. The Sigi Regency in general has both of these potentials, as an unstable zone as well as having many hot springs as a manifestation of geothermal potential. Hopefully the results of this research can contribute information and be a consideration for local governments in making future urban planning.

3. MATERIALS AND METHOD

The gravity method measures variations in the rock density of a subsurface rock. In this method, it is necessary to make some corrections to the gravity data because the observed gravity value is influenced by latitude, elevation, terrain topography, earth tides, and variations in subsurface rock density [30]. Gravity data in this study is used from ground survey primary data acquired by Central Agency for Coal and Geothermal Mineral Resources Indonesia. There are 256 stations of gravity measurement that are spreading into 7 lines which are focused on the main area and the others randomly distributed around it. The distance between stations is 250 m, while the distance between lines is about 1 km. As shown in Fig. 1, there are right Palu Koro Fault (east), left Palu Koro Fault (west), and Fault Br in this study area.

The MS-SVD is a method that can be used to determine the presence and characteristics of a structure. This method is applying the SVD method to the up-warding continuation of gravity anomaly in several continuation levels [29, 31]. The MS-SVD method can be described as a band-pass filter. SVD calculations are carried out based on the Laplace equation so that the second derivative of gravity is obtained as in the following equation [32],

$$\frac{\partial^2 g}{\partial z^2} = -\left(\frac{\partial^2 g}{\partial x^2} + \frac{\partial^2 g}{\partial y^2}\right) \tag{1}$$

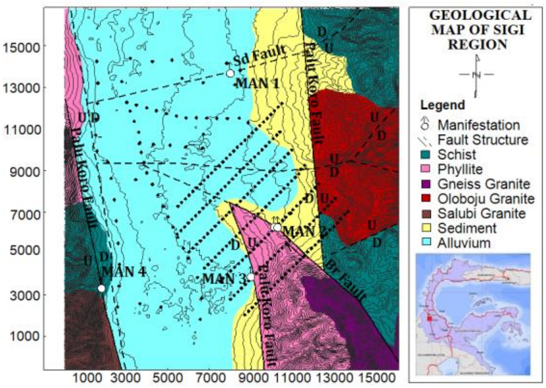

Fig.1 Geological map of Sigi Regency and gravity stations that are spread in 7 lines and its surrounding.

This study begins with the correction of gravity data from latitude correction to terrain correction to obtain the complete Bouger anomaly (CBA) value. Then the regional and residual anomalies are separated with upward continuation. Furthermore, the derivative analysis uses FHD and SVD to determine the presence and type of fault in this area. The next step of SVD is MS-SVD analysis which aims to further characterize the fault structure. In the MS-SVD process, upward continuation (UC) is performed on CBA data at various different heights. At each altitude, SVD is performed against the resulting UC. Fault location points obtained from MS-SVD at each elevation are then plotted on an upward elevation curve (*h*) versus the fault position (*x*). From the results of this plotting obtained the direction as well as the angle of the dip.

4. RESULTS AND DISCUSSION

The topography of the field is fairly varied, its elevation ranges from 20.13 masl to 440.76 masl. The existence of an elevation difference around the gravity station influences the value of gravity readings on the gravimeter. The observed gravity value is need to be corrected by terrain correction, so then obtain a CBA value. The CBA map in Fig. 2 shows anomaly values with an interval of -25.79 mGal to 7.55 mGal. The map is overlaid on top of the regional geological map.

The contrast boundary of the CBA anomaly shows a lineation with a North-South direction that indicates the presence of two tectonic structures of the Palu Koro Fault. It has a relatively North-South trending strike direction. The two main structures form a graben on the middle part, with a lower anomaly on the Southside than on the North ones. The presence of this graben was also stated by Patria and Putra [8]. While the lower anomaly is due to the basement rock deepening on both sides, the North and South part is low anomaly areas. The low value of gravity in the North is thought to be related to the initiation of subduction that occurred in the northern part of the Palu Koro Fault [33]. However, the basement deepening that occurs on the Northside is still shallower than on the South part [34].

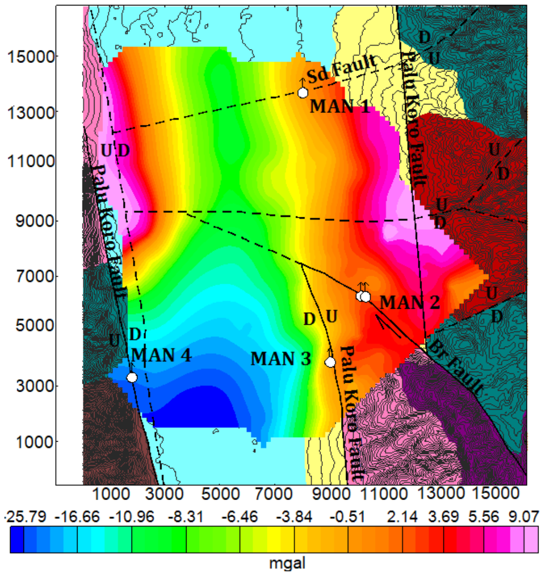

Fig.2 CBA (complete Bouger anomaly) map result that is overlaid with geological map.

Determination of the regional anomaly of the CBA is obtained from the upward continuation process of the CBA contour map. In this study, a regional anomaly map was obtained from the continuation at level 1000m as shown in Fig. 3. Regional anomaly is influenced by deep regional rocks. The basement rock in this field is thought to be schist rock that almost covers the entire basement of this field and is estimated to be at a depth of about 1000m [34]. There is a high anomaly contour such as intrusion of Oloboju granite that breaks through

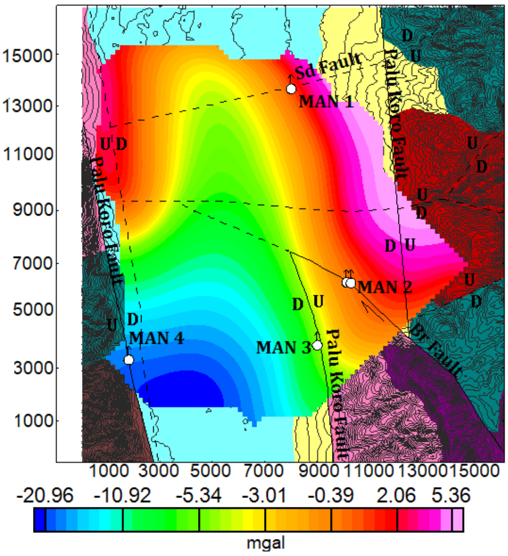

Fig.3 Gravity regional anomaly map that is overlaid with geological data.

the surface on the East side of this field and metamorphic rocks on the Northwest side. While the low anomaly on the middle part is a graben which has a deeper depth on the Southside.

The residual anomaly map in Fig. 4 has a range of anomaly values of -5.64 mGal to +5.20 mGal. The low anomaly that extends to the North-South direction is strongly suspected due to the influence of sedimentary and alluvial rocks that fill the graben to the surface. On the residual map, the low anomaly contour on the Northside of the graben area is lower than on the CBA anomaly map. This low anomaly in the North and South is separated by a green contour with a value of -1 mGal to -2.67 mGal. The low anomaly in the North seems to have a boundary separated by a West-East geological structure. The contour boundary of the North low anomaly is relatively tangent to the presence of the Fault Sd of the geological data [6]. It is suspected that the Fault Sd is a boundary of the low anomaly in the North. Meanwhile, the geological data does not show any fault that may correlate with a boundary of the low anomaly in the South.

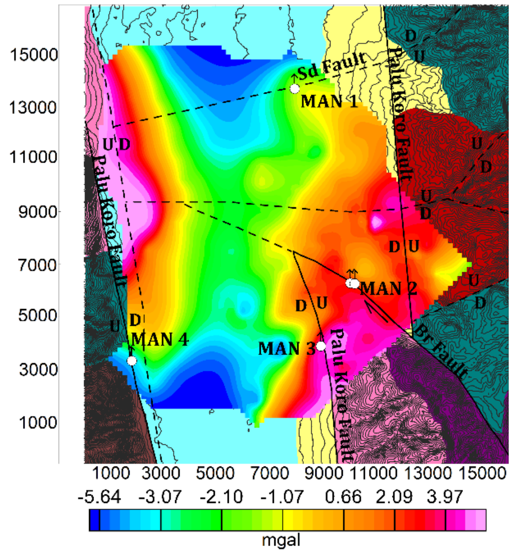

Fig.4 Residual gravity anomaly map that is overlaid with geological map.

The FHD contour map was processed from the contours of the residual anomaly. Its values ranged from 0.00036 mGal/m to 0.00555 mGal/m. The FHD contour map shows the maximum value as the density contrast boundary [28]. Then the indication of the existence of the structure is marked by the maximum anomaly value that forms the straight line. The estimation of the existence of the fault structure still needs to be strengthened by structural analysis from the SVD map. The zero values of SVD contour can be used to determine the structure which forms a straight line in the same position as the results of the structural analysis from the FHD map. From both derivative analyses (FHD and SVD), the estimated fault line is marked by a thick black line with a fault label as shown in Fig. 5.

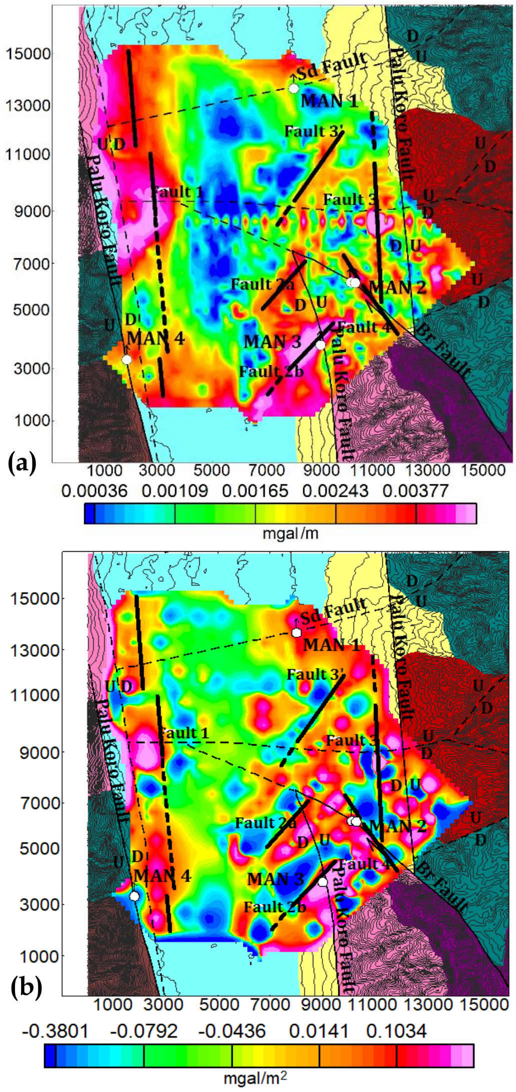

Fig.5 (a) FHD and (b) SVD map with fault lines estimation in bold black lines.

Based on the results of the analysis of the FHD and SVD filters, five faults were obtained namely Fault 1, Fault 2, Fault 3, Fault 3', and Fault 4 (see Fig. 5). Fault 2 is separated into 2 fault segments i.e. Fault 2a and Fault 2b. The separation of Fault 2 into 2 segments makes a hypothesis of an unknown geological structure with an East-West trend. The situation is supported by the presence of a low anomaly boundary in the South of the residual anomaly map and Fault 1 which is cut off and shifted into the East. In addition, the FHD and SVD analysis show an estimated fault that is not found on the geological map, namely Fault 3'. It is suspected that Fault 3' originally formed a fault line with Fault 2a and Fault 2b with a strike line in an almost North-South direction. The fault which is in the weak zone of graben depression is then cut into 3 parts (Fault 3', Fault 2a, and Fault 2b) by a shear fault trending East-Southeast of the Fault Br. This Fault Br is not well identified by gravity data because it is a strike-slip fault, but it is well mapped on geological data of Wibowo et al. [6]. It is also verified by Nugraha et al. [35] that stated the faults in Palu surroundings are predominantly controlled by strike-slip or horizontal fault mechanisms. The strike directions of the three fault segments (Fault 3', Fault 2a, and Fault 2b) which are currently trending Northeast-Southwest are also thought to be due to the shear drag of Fault Br which moves to the Southeast. After the 2018 Palu events, the fault zone is dominated by normal and strike slip faults with NNE-SSW trend [36]. The fault branches into multiple semi-parallel fault segments toward shallower depth which the displacement is generally larger east of the fault [37].

MS-SVD analysis is carried out by upwards continuation at several levels, then deriving with SVD at each level. In this study, the upward continuation of the CBA value was carried out at 7 level variations, they are 300m, 600m, 900m, 1200m, 1500m, 1800m, and 2000m. For each estimated fault line, SVD values are sliced from all continuation levels on the slicing line which is perpendicular to the estimated fault line. The slicing line is marked by a white line in Fig. 6, even on FHD values are sliced on the same line.

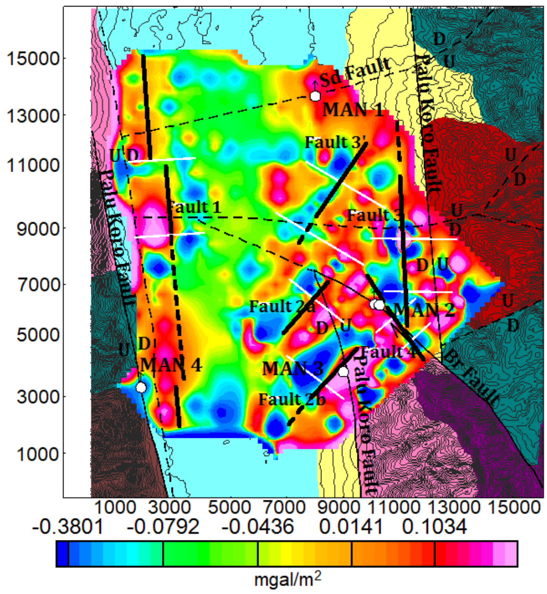

Fig.6 SVD map with slicing line on fault line estimation for further fault characterization.

The data on each slicing line is then plotted into FHD and SVD correlation curves, and at the same point, it is matched with the MS-SVD vs coordinates curve. FHD and SVD correlation curves to determine the exact point of the fault are shown by the maximum value of FHD and zero value of SVD as has been well demonstrated by Rosid et al. [38]. The MS-SVD curve vs coordinates is used to find out the magnitude and direction of the dip angle of the fault.

From the MS-SVD correlation graph, the characteristics of each fault can be identified and summarized in Table 1. In the table, UC is Upward Continuation level, the depths are obtained from conversion UC level to estimation depth by Rosid and Naufal equation (unpublished). Distance *R* is coordinate, and it started from zero to show its distance for each depth. Fault dip is known from curve distance (*R*) vs depth. The magnitude of the fault dip angle is obtained by calculating the tangent angle of the trendline slope of the curve. Based on MS-SVD analysis, Fault 1 is indicated as the left Palu Koro Fault which on the geological map extends on the west side, that is a normal oblique fault type. This fault has an average dip of 85.4° eastward. This study area is an extensional zone, where there is a graben formed between the left and right couple of Palu Koro Faults.

As Fault 1 becomes the left Palu Koro Fault of the graben, then the right Palu Koro Fault is Fault 2 and Fault 3 which were previously conjugated but have been separated by Fault 4. The characteristics of Fault 2 and Fault 3 also have similarities of dip oriented which are relative to the West. Both have the opposite direction to Fault 1 and the magnitude of the dip of the three faults is also relatively similar, which is around 85°. The dip value is near-vertical [37].

Two segment of Fault 2 which is separated into Fault 2a and 2b is due to the influence of Fault 4 movement. Apart from being separated into two parts, the position and strike direction of the two fault segments are relatively irregular. Fault 2, which was previously part of Fault 3, ideally has the same strike direction as Fault 3, that is the North-South direction. However, based on SVD analysis, the strike direction of Fault 2 changes to the Southwest-Northeast.

Fault 4 is suspected as Fault Br on the geological map. This fault is separating the right Palu Koro Fault into two parts (Fault 2 and 3) and changes the strike direction of Fault 2. It is also suspected of causing a dragging effect then Fault 3' was formed. This happens because Fault 4 is a dextral shear fault, where the block shifting to the southeast produces a local extensional zone and forms a normal fault of Fault 3'. It was also verified by Supartoyo et al. [39] which says that the Palu Koro Fault is divided into 7 segments. However, all faults from MS-SVD are related to the existence of faults in the geological map except Fault 3'. So that, Fig. 7 is the map of these faults with the symbol D-U, in which D is down for the hanging wall.

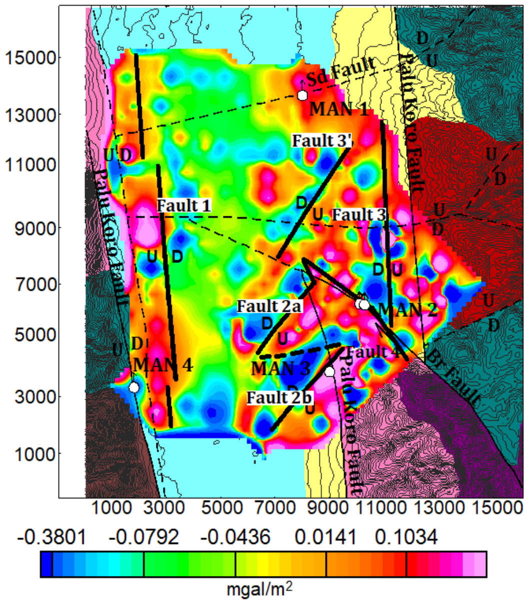

Fig.7 Map of fault distribution from MS-SVD analysis with dip direction.

Table 1. Fault characterization based on MS-SVD result.

UC level	Depth (m)	*R* (m) Fault 1a	Fault 1b	Fault 2a	Fault 2b	Fault 3a	Fault 3b	Fault 4a	Fault 4b	Fault 3'a	Fault 3'b
0	7.01	0	0	0	0	0	0	0	0	0	0
300	261.86	17	12	0	11.16	-13	3.04	114	136.02	-17.47	94
600	532.91	39	30	10.63	11.16	-	-1.57	-	285.62	2.96	128
900	820.16	65	51	42.72	44.63	-	-	-	-	18.56	128
1200	1123.61	84	72	53.45	89.26	-	-	-	-	21.23	128
1500	1443.26	104	88	53.45	144.94	-	-	-	-	13.4	111
1800	1779.111	118	103	31.99	211.88	-	-	-	-	10.66	103
2000	2012.011	127	112	21.36	245.36	-	-	-	-	6.4	94
Max		1	1	1	1	1	1	1	1	1	1
Min		-0.2235	-0.6296	-0.4806	-0.7784	-0.2434	-0.3861	-0.5601	-0.2486	-0.4806	-0.6555
Type		Normal	Normal	Normal	Normal	Normal	Normal	Normal	Normal	Normal	Normal
Dip Angle		85.166	85.755	86.97	80.71	87.45	88.17	86.74	81.87	81.12	79.91
Dip Direction		East	East	Northwest	Northwest	West	West	Northeast	Northeast	Northwest	Northwest

5. CONCLUSION

Based on the results of the analysis and interpretation of the gravity method and the correlation with supporting data to identify the characteristics of the structure in this study area, it can be concluded that:

- The MS-SVD gravity analysis identified 5 normal faults or normal oblique structures which were strongly correlated with and verified by the geological data scattered in this study area.
- Fault 1, Fault 2, and Fault 3 in the results of the derivative analysis are normal oblique faults that are an indication of the Palu Koro Fault. While Fault 4 is a normal oblique fault which is an indication of the Fault Br on the geological map.
- The dynamics of the fault structure resulted in a derivative analysis of faults that did not exactly match the faults on the geological map, as Fault 2 is known to be divided into 2 segments Fault 2a and Fault 2b.
- Fault 3' was found to be a normal fault formed in the weak zone and as a result of dragging by Fault 4 (Fault Br).

6. ACKNOWLEDGMENTS

On this occasion, the authors would like to thank the Bandung Geothermal Coal Mineral Resource Center for allowing us to use this gravity data to conduct studies and publish the subsurface structures in the Sigi Regency area. Thanks also to the Faculty of Mathematics and Natural Sciences, Universitas Indonesia for their valuable financial assistance through the FMIPA 2021 research grant No. NKB-021/UN2.F3/HKP.05.00/2021 to support this publication process.

7. REFERENCES

[1] Hall, R. (1996). Reconstructing Cenozoic SE Asia. In R. Hall, & D. J. Blundell (Eds.),, Eds., Tectonic evolution of SE Asia, Vol. 106, pp. 153–184. Geological Society, London, Special Publications. https://doi.org/10.1144/GSL.SP.1996.106.01.11

[2] Walpersdorf, A., Vigny, C., Subarya, C., and Manurun, P. (1998). Monitoring of the Palu-Koro Fault (Sulawesi) by GPS. Geophysical Research Letters, Vol. 25, No.13, p. 2313-2316.

[3] Bellier, O., Sébrier, M., Beaudouin, T., Villeneuve, M., Braucher, R., Bourles, D., Siame, L., and Pratomo, I. (2001). High slip rate for a low seismicity along the Palu-Koro active fault in central Sulawesi (Indonesia). Terra Nova, 13(6), p. 463-470. https://doi.org/10.1046/j.1365-3121.2001.00382.x

[4] Socquet. A., Simons, W., Vigny, C., McCaffrey, R., Subarya, C., Sarsito, D., Ambrosius, B., and Spakman, W. (2006). Microblock rotations and fault coupling in SE Asia triple junction (Sulawesi, Indonesia) from GPS and earthquake slip vector data. Journal of Geophysical Research: Solid Earth. 111 (B8). https://doi.org/10.1029/2005JB003963

[5] Massinai, M. F. I., Ariansyah, M. R., Trisartika, R., and Massinai, M. A. (2020). Relative present-day motion on Palu-Koro Fault. IOP Conf. Ser.: Earth Environ. Sci. 575 012185. DOI: /10.1088/1755-1315/575/1/012185

[6] Wibowo, A. E., Hermawan, D., and Widodo, S. (2010). Penyelidikan Terpadu Geologi dan Geokimia Daerah Panasbumi Bora Kabupaten Sigi Provinsi Sulawesi Tengah. Work report, Pusat Sumber Daya Geologi Bandung.

[7] National Earthquake Study Center Team. (2018). The Study of the Palu Earthquake, Central Sulawesi Province 28 September 2018 (M7.4). Research and Development Center of the Ministry of Public Works and Public Housing.

[8] Patria, A., and Putra, P. S. (2020). Development of the Palu–Koro Fault in NW Palu Valley, Indonesia. Geoscience Letters, Vol. 7, no. 1. https://doi.org/10.1186/s40562-020-0150-2

[9] Leopatty, H., Efendi, R., Rande, M. N., Asyhar, I. F., and Cholidani, M. (2021). Identification of Earthquake Shake Levels in Sigi Regency Based on Mw 6,9 Shakemap Scenario by Palu Koro Fault. Gravitasi, 20(2), p. 42-46. https://doi.org/10.22487/gravitasi.v20i2.15552

[10] Rosid, M.S., Ali, Y.H., and Ramdhan, M. (2022). Characterization of the Mamasa Earthquake Source Based on Hypocenter Relocation and Gravity Derivative Data Analysis. International Journal of GEOMATE, Sept. 2022, Vol.23, Issue 97, pp.220-227. DOI: https://doi.org/10.21660/2022.97.j2375.

[11] Liu, C., and Shi, Y. (2021). Space-time stress variations on the Palu-Koro fault impacting the 2018 Mw 7.5 Palu earthquake and its seismic hazards. Geochemistry, Geophysics, Geosystems, 22, e2020GC009552. https://doi.org/10.1029/2020GC009552

[12] BMKG (Badan Meteorologi, Klimatologi, dan Geofisika). (2020). BMKG earthquakes repository 2012. http://repogempa.bmkg.go.id/repo_new/viewmap.php?tgl=2012/08/18&ot=09:41:53.654&l

at=1.26&lon=120.13&ketlat=S&ketlon=E&depth=10&mag=6.2&remark=Sulawesi%2C+Indonesia+&status=unset.
And BMKG earthquakes repository 2020. http://repogempa.bmkg.go.id/repo_new/viewmap.php?tgl=2020/03/28&ot=15:43:18.442&lat=1.70&lon=120.15&ketlat=S&ketlon=E&depth=13&mag=5.9&remark=Sulawesi%2C+Indonesia+&status=unset.

[13] Kasbani, K. (2009). Types of Geothermal Systems in Indonesia and Estimated Energy Potential. Geological Resources Bulletin, 4(3), p. 23-30.

[14] Idral, A. (2010). Potency of Non-Volcanic Hosted Geothermal Resources in Sulawesi-Indonesia. Proceedings World Geothermal Congress 2010, Bali, Indonesia, 25-29 April 2010.

[15] Suparman, Sulastri, M., and Andriany, S.S. (2015). Wells Declivity Temperature Geothermal Field Bora-Sigi, Central Sulawesi, Indonesia. In: Lollino G., Manconi A., Clague J., Shan W., Chiarle M. (eds) Engineering Geology for Society and Territory - Volume 1, pp. 373-378. Springer, Cham. https://doi.org/10.1007/978-3-319-09300-0_71

[16] Putriyana, L., Daud, Y., Saha, B. D., and Nasruddin, N., (2022). A comprehensive data and information on low to medium temperature geothermal resources in Indonesia: a review. Geomech. Geophys. Geo-energy. Geo-resource., (2022) 8:58. https://doi.org/10.1007/s40948-022-00375-5

[17] Sumantoro, Z. Z., Yeh, A., O'Sullivan, J. P., and O'Sullivan, M. J. (2015). Reservoir Modelling of Lahendong Geothermal Field, Sulawesi – Indonesia. Proceedings 37th New Zealand Geothermal Workshop 18 – 20 November 2015, Taupo, New Zealand.

[18] Agustina, L., and Suyanto. (2020, July). The low-medium enthalpy geothermal power plant at Lahendong, Indonesia. In AIP Conference Proceedings, Vol. 2248, No. 1, p. 060001. AIP Publishing LLC.

[19] Zarkasyi, A., Rahadinata, T., Suhanto, E., and Widodo, S. (2015, April). Investigation of geothermal structures of the Kadidia Area, Indonesia, using the magnetotelluric method. In Proceedings world geothermal congress, Melbourne, Australia (pp. 19-25).

[20] Dwiputra, G. P., Rangkuti, N. S., Yoni, D. R., and Zakaria, Z. (2017). Model Hidrogeologi dan Sistem Panas Bumi Daerah Koala Rawa, Kabupaten Sigi, Sulawesi Tengah. Proceeding, Seminar Nasional Kebumian ke-10, 13 – 14 September 2017; Graha Sabha Pramana. p. 1463 – 1475.

[21] Zarkasyi, A., and Nurdin, N.M. (2018). Survei Magnetotelurik dan TDEM Daerah Panas Bumi Kadidia – Kadidia Selatan, Kabupaten Sigi, Provinsi Sulawesi Tengah. Prosiding Hasil Kegiatan Pusat Sumber Daya Geologi Tahun 2014, No. 9.
DOI: https://doi.org/10.31219/osf.io/ev7gw

[22] Nurdin, N.M. (2013). Zona prospek panas bumi daerah Kadidia, Kabupaten Sigi, provinsi Sulawesi Tengah berdasarkan data magnetotellurik. Skripsi. Universitas Padjadjaran, Bandung. http://repository.unpad.ac.id/frontdoor/index/index/docId/126558

[23] Sijabat, E. (2021). Identifikasi struktur patahan dalam penetuan reservoar bumi menggunakan data gayaberat pada daerah Kadidia Selatan Provinsi Sulawesi Tengah. Skripsi. Teknik Geofisika, Institut Teknologi Sumatera, Lampung. http://perpustakaan.itera.ac.id/slims/index.php?p=show_detail&id=5813

[24] Rachmatika, D. (2019). Karakteristik zona mineral alterasi pada lapangan panasbumi Kadidia, Kabupaten Sigi, Provinsi Sulawesi Tengah. Skripsi. Universitas Padjadjaran, Bandung. http://repository.unpad.ac.id/frontdoor/index/index/docId/38929

[25] Wibowo, A.E.A., Nurhadi, M., Rezky, Y., Herma-wan, D., and Setiawan, D.I. (2015). Penentuan Kesamaan Reservoar Sistem Panas Bumi Kadidia dan Kadidia Selatan Kabupaten Sigi, Provinsi Sulawesi Tengah Berdasarkan Metoda Geokimia. Buletin Sumber Daya Geologi, Vol. 10 No. 2. http://buletinsdg.geologi.esdm.go.id/index.php/bsdg/article/view/BSDG_VOL_10_NO_2_2015_4

[26] Firmansyah, I., Siswandi, Iswahyudi, S., Hermawan, D., and Mustofa, S. A. (2022). The detailed geological investigation in Kadidia geothermal areas, Nokilalaki District, Sigi Regency, Central Sulawesi Province. Journal of Earth and Marine Technology (JEMT), 2(2), p. 92 – 98. https://doi.org/10.31284/j.jemt.2022.v2i2.2870

[27] Abdullah, A. I., Puspita, R., and Hamad, H. (2019). Review of Regional Geological Structures on the Appearance of Geothermal Manifestations in the "Neck" Region of Western Sulawesi Island. MATEC Web of Conferences 331, 03003 (2020). https://doi.org/10.1051/matecconf/202033103003

[28] Rosid, M. S. and Siregar, H. (2017). Determining fault structure using first horizontal derivative (FHD) and horizontal

vertical diagonal maxima (HVDM) method: A comparative study. AIP Conference Proceedings 1862, 030171. http://dx.doi.org/10.1063/1.4991275.

[29] Yudyawati, K. N., and Rosid, M. S. (2020). Identification the Jakarta Fault using MS-SVD (Multi Scale-Second Vertical Derivatives) Method Gravity Data. In IOP Conference Series: Materials Science and Engineering, Vol. 854, No. 1, p. 012044. https://doi.org/10.1088/1757-899X/854/1/012044.

[30] Telford, W. M., Geldart, L. P., and Sheriff, R. E. (1990). Applied Geophysics. Cambridge University Press.

[31] Naufal, M. A., and Rosid, M. S. (2020, May). Structure identification of geothermal field "X" using ML-SVD method of gravity data. In IOP Conference Series: Materials Science and Engineering, 854 (1), p. 012055. https://doi.org/10.1088/1757-899X/854/1/012055.

[32] Blakely, R. J. (1996). Potential theory in gravity and magnetic applications. Cambridge University Press.

[33] Zhang, J., Hao, T., Dong, M., Xu, Y., Wang, B., Ai, Y., and Fang, G. (2021). Investigation of geothermal structure of the Sulawesi, using gravity and magnetic method. Sci. China Earth Sci. 64, p. 278–293 (2021). https://doi.org/10.1007/s11430-020-9659-3

[34] Zulfafa, D. (2016). Identification of Geological Structures with Horizontal Gradient Analysis and Euler Deconvolution Based on Gravity Data. Lampung: Universitas Lampung.

[35] Nugraha, J., Jaya, A., and Alimuddin, I. (2019). Identification of Palu-Koro Fault Mechanism and Earthquake Hazard Vulnerability of Palu Area Central of Sulawesi. International Journal of Engineering and Science Applications. 6 (2), p. 48 – 59.

[36] Anugrahadi, A., Sumarto, U., and Purwiyono, T. T. (2021). The Palu Earthquake Formed a New Geological Structure. IOP Conf. Series: Earth and Environmental Science 819 (2021) 012027. https://doi.org/10.1088/1755-1315/819/1/012027

[37] Simons, W., Broerse, T., Shen, L., Kleptsova, O., Nijholt, N., Hooper, A., et al. (2022). A tsunami generated by a strike-slip event: Constraints from GPS and SAR data on the 2018 Palu earthquake. Journal of Geophysical Research: Solid Earth, 127, e2022JB024191. https://doi.org/10.1029/2022JB024191

[38] Rosid, M. S., Tullailah, N. N., and Wibowo, R. A. (2020). Identifikasi potensi jebakan hidrokarbon di daerah cekungan Sumatra Utara menggunakan data gravitasi. Jurnal Fisika, 10 (1) (2020), p. 8 – 21. https://journal.unnes.ac.id/nju/index.php/jf/article/view/23955

[39] Supartoyo, S., Sulaiman, C., and Junaedi, D. (2014). Kelas Tektonik Sesar Palu Koro, Sulawesi Tengah. Jurnal Lingkungan dan Bencana Geologi, Vol. 5 No. 2 Agustus 2014: 111 – 128. DOI: http://dx.doi.org/10.34126/jlbg.v5i2.68